Title

β-D-N^4-hydroxycytidine, a metabolite of molnupiravir, exhibits *in vitro* antiviral activity against rabies virus

Authors: Kei Konishi[1,2], Shinji Kusakabe[1,2], Nijiho Kawaguchi[3], Takao Shishido[1], Naoto Ito[4], Michiko Harada[5], Satoshi Inoue[5], Ken Maeda[5], William W. Hall[6,7,8,9], Yasuko Orba[2,3,6,9,10], Hirofumi Sawa[2,6,8,9,10], Michihito Sasaki[3,9]* and Akihiko Sato[1,2,9]*

Affiliations: [1] Laboratory for Drug Discovery & Disease Research, Shionogi & Co., Ltd., Osaka, Japan

[2]Division of Anti-Virus Drug Research, International Institute for Zoonosis Control, Hokkaido University, Sapporo, Japan

[3]Division of Molecular Pathobiology, International Institute for Zoonosis Control, Hokkaido University, Sapporo, Japan

[4]Laboratory of Zoonotic Diseases, Faculty of Applied Biological Sciences, Gifu University, Gifu, Japan

[5]Department of Veterinary Science, National Institute of Infectious Diseases (NIID), Tokyo, Japan

[6]International Collaboration Unit, International Institute for Zoonosis Control, Hokkaido University, Sapporo, Japan

[7]National Virus Reference Laboratory, School of Medicine, University College of Dublin, Ireland

[8]Global Virus Network, Baltimore, Maryland, USA

[9]Institute for Vaccine Research and Development (HU-IVReD), Hokkaido University, Sapporo, Japan

[10]One Health Research Center, Hokkaido University, Sapporo, Japan

*Corresponding author:

Akihiko Sato, E-mail: akihiko.sato@shionogi.co.jp

Michihito Sasaki, E-mail: m-sasaki@czc.hokudai.ac.jp

Abstract

Rabies is a fatal neurological disorder caused by rabies virus (RABV) infection. Approximately 60,000 patients die from rabies annually, and there are no effective treatments for this disease. Nucleoside analogs are employed as antiviral drugs based on their broad antiviral spectrum, and certain nucleoside analogs have been reported to exhibit anti-RABV activity. The nucleoside analog β-D-N^4-hydroxycytidine (NHC) has antiviral effects against a range of RNA viruses. Molnupiravir (MPV), a prodrug of NHC, is clinically used as an oral antiviral drug for coronavirus infections. Despite its broad-spectrum activity, the antiviral activity of NHC against RABV remains unclear. In this study, we reveal that NHC exhibits comparable *in vitro* anti-RABV activity as ribavirin and favipiravir (also known as T-705) with a 90% effective concentration of 6 μM in mouse neuroblastoma cells. NHC reduced viral loads in neuronal and nonneuronal cells in a dose-dependent manner. Both laboratory and field RABVs (fixed and street strains, respectively) were susceptible to NHC. However, no increase in survival or reduction in viral titers in the

brain was observed in RABV-infected mice treated prophylactically with MPV. These findings highlight the potential and challenges of NHC in the treatment of RABV infection.

Keywords (a maximum of 6 keywords)

Rabies virus, antiviral, β-D-N^4-hydroxycytidine, Molnupiravir, Nucleoside analog

Abbreviations: RABV, rabies virus; SARS-CoV-2, severe acute respiratory syndrome coronavirus 2; COVID-19, coronavirus disease 2019; NHC, β-D-N^4-hydroxycytidine; MPV, molnupiravir; RBV, ribavirin; T-705, favipiravir; PEP, post-exposure prophylaxis

Highlights

- β-D-N^4-hydroxycytidine (NHC) exhibited antiviral activity and inhibited rabies virus (RABV) infection in cultured cells.
- NHC had a comparable 90% effective concentration as ribavirin and T-705 in cultured cells.
- No therapeutic effect was observed for oral molnupiravir, a prodrug of NHC, in RABV-infected mice.

1. Introduction

Rabies virus (RABV) is an RNA virus belonging to the order *Mononegavirales*, family *Rhabdoviridae*, and genus *Lyssavirus*. RABV is transmitted to humans through biting by RABV-infected animals. Following the establishment of infection, RABV invades the

central nervous system (CNS), and the fatality rate of rabies is almost 100% once neurological symptoms develop. It is estimated that approximately 60,000 individuals succumb to this disease annually(Fooks et al., 2017) . The standard treatment of rabies is post-exposure prophylaxis (PEP), involving the administration of a vaccine against RABV and human RABV immunoglobulin. However, the accessibility of PEP is often limited in areas with a high prevalence of rabies (Henry et al., 2022; Sreenivasan et al., 2019) because of high costs and hurdles both in distribution and storage. It has been reported that one patient recovered from rabies by receiving a therapeutic coma and a combination treatment with ketamine, midazolam, ribavirin (RBV), and amantadine, known as the Milwaukee Protocol (Willoughby et al., 2005). However, the effect of treatment has rarely been reproduced and remains to be doubtful since only one of ten patients who received the Milwaukee Protocol survived from 2015 to 2022 (Arslan and Vahaboglu, 2023; Zeiler and Jackson, 2016). In conclusion, there is no established treatment for patients who develop symptoms of rabies. Given these constraints, further treatment options against infection are urgently required.

Nucleoside analogs comprise a class of small-molecule antiviral drugs. These antiviral drugs mimic host nucleosides and interfere with the activity of the viral RNA-dependent RNA polymerase (RdRp), a key enzyme in viral replication. Because RdRp is highly conserved across viral species, nucleoside analogs are known to exhibit broad-spectrum antiviral activity (Geraghty et al., 2021; Venkataraman et al., 2018). Certain nucleoside analogs are clinically used as antiviral drugs for infectious diseases, such as remdesivir for coronavirus disease 2019 (COVID-19) and sofosbuvir for hepatitis C (Beigel et al., 2020;

Lawitz et al., 2013). Within the context of rabies, the nucleoside analogs RBV and favipiravir (also called T-705) have been reported to exhibit anti-RABV activity(Du Pont et al., 2019). Although RBV inhibited RABV infection *in vitro*, efficacy *in vivo* has not been proven (Anindita et al., 2018; Bussereau et al., 1988). Indeed, despite its clinical usage, the effectiveness of RBV remains controversial (Appolinario and Jackson, 2015). Monotherapy with T-705 was effective but insufficient to ameliorate the disease conditions of rabies in preclinical studies (Banyard et al., 2019; Kimitsuki et al., 2023; Yamada et al., 2016). These findings highlight the need for more effective nucleoside analogs for rabies virus treatment.

β-D-N^4-hydroxycytidine (NHC), an active metabolite of molnupiravir (MPV), is a nucleoside analog, and MPV was originally developed for treatment of seasonal influenza. With the emergence of the COVID-19 pandemic, MPV was instead approved as the first oral antiviral agent for COVID-19 (Imran et al., 2021; Jayk Bernal et al., 2022). MPV is authorized for use in more than 25 countries, however, it has relatively low efficacy in COVID-19, and there are concerns about its risk for mutagenesis, which could lead to the production of mutant viruses (Butler et al., 2023; Sanderson et al., 2023). In addition to its activity against severe acute respiratory syndrome coronavirus 2 (SARS-CoV-2) and influenza virus, NHC has also displayed antiviral activity against a variety of RNA viruses, including Chikungunya virus, Venezuelan equine encephalitis virus (VEEV), Ebola virus, and Respiratory Syncytial virus, indicating a broad antiviral spectrum (Bluemling et al., 2023; Downs et al., 2023; Ehteshami et al., 2017; Painter et al., 2019; Urakova et al., 2018; Yoon et al., 2018). However, there have been no studies on the efficacy of NHC against

RABV. In this study, we have investigated the anti-RABV activity of NHC in both *in vitro* and *in vivo* models.

2 Materials and Methods

2.1 Cells and viruses

The mouse neuroblastoma cell line N2a (IFO50081) and hamster kidney fibroblast line BHK-21/C-13 (JCRB9020) were obtained from the JCRB Cell Bank (Osaka, Japan). SK-N-SH human neuroblastoma cells (RCB0426) were obtained from the Riken BioResource Research Center. NA mouse neuroblastoma cells were as described previously (Sugiyama et al., 2002). All cell lines were maintained in Eagle's Minimum Essential Medium (EMEM) containing 10% fetal bovine serum (FBS).

The fixed RABV strains CVS and HEP and the street RABV strain Toyohashi (Nosaki et al., 2021) were propagated in NA cells. Viral titers were determined by a focus-forming assay as described previously (Anindita et al., 2018). The mouse-adapted SARS-CoV-2 strain (MA-P10) was established from the SARS-CoV-2 WK-521 strain (lineage A, GISAID ID: EPI_ISL_408667) and viral titers were determined using the 50% tissue culture infectious dose ($TCID_{50}$) assay as described previously (Uemura et al., 2023). All viruses were stocked at −80°C until experimental use.

2.2 Compounds

NHC was purchased from the Tokyo Chemical Industry Co., Ltd. (H1803). MPV was purchased from Angene (AN-AG01V2KZ). T-705 was also purchased from Angene (AG002R9Q). RBV was purchased from Wako Chemical Industries, Ltd. (188-02333). GRP-60367, a RABV entry inhibitor, was purchased from MedChemExpress (HY-133735A). All compounds were initially dissolved in dimethyl sulfoxide (DMSO) for the *in vitro* experiments. For *in vivo* experiments, compounds were prepared as described in the animal experimental section.

2.3 Cell viability assay

Cells seeded into 96-well plates were incubated with NHC, T-705, or RBV. All compounds were serially diluted twofold in EMEM containing 2% FBS. After 2 days of culture, cells were stained with 3-(4,5-dimethylthiazol-2-yl)-2,5-diphenyltetrazolium bromide (MTT) and lysed with 2-propanol containing 10% Triton X and 0.28% HCl. Cell viability was then calculated according to the percent absorbance of cells treated with the compounds. The absorbance of cells treated with 0.4% (v/v) DMSO served as the baseline for 100% cell viability.

2.4 Evaluation of antiviral efficacy in various cell lines by viral titer

Cells seeded in 24-well plates were inoculated with RABV-HEP or RABV-CVS at a multiplicity of infection (MOI) of 0.01 or RABV-Toyohashi at a MOI of 0.1. After incubation with the viral inoculum for 1 h at 37°C, cells were

cultured with compound-containing medium. Culture supernatants were collected at 48 h post infection (hpi) and subjected to virus titration by the focus-forming assays. The 90% effective concentrations (EC_{90}s) were calculated as the concentration at which the viral titer was reduced by 90% relative to the non-treated control.

2.5 **Quantitative RT-PCR**

NA cells were infected with RABV-CVS at a MOI of 0.01 for 1 h, and the viral inoculum was replaced with EMEM supplemented with 2% FBS and NHC. At 48 hpi, total RNA was extracted using a Direct-Zol RNA MiniPrep kit (Zymo Research). qRT-PCR was conducted using a Thunderbird Probe One-step qRT-PCR Kit (Toyobo) and StepOnePlus Real-Time PCR Systems (Applied Biosystems). The viral copy number was measured by the standard curve method. The primers and probes for the RABV-CVS N gene used were as previously described (Itakura et al., 2023).

2.6 **Immunofluorescence assay**

NA cells were infected with RABV-CVS at a MOI of 0.01. Following 1 h of incubation, cells were cultured in the presence of NHC. NA cells at 48 hpi were fixed with 3.7% formaldehyde in PBS and incubated with staining solution (PBS containing 0.2% Triton X-100, 25% Block Ace, 0.4% FITC-conjugated anti-RABV N antibody [Fujirebio Diagnostics, Inc], and 1% Hoechst 33342

178 [Invitrogen]). Fluorescent images were captured using an IX73 fluorescence
179 microscope (Olympus).
180
181 2.7 **Time-of-addition assay**
182 RABV-CVS was preincubated with or without compounds at 37°C for 1 h.
183 Each virus–compound mixture or virus alone was then inoculated into N2a cells
184 at a MOI of 0.01. At 1 hpi, the cells were washed twice with EMEM containing
185 2% FBS and cultured in the presence (post-entry treatment) or absence (pre-entry
186 treatment) of each compound. Viral RNA was extracted at 16 hpi, and the
187 relative viral RNA expression was analyzed by qRT-PCR using the ΔΔCt
188 method. Mouse *Actb* was used as an endogenous control. The primer and probe
189 sequences of mouse *Actb* were designed using a PrimeTime qPCR assay
190 (Integrated DNA Technologies). The primers and probes for RABV-CVS were
191 as described above.
192
193 2.8 ***In vitro* combination assay of NHC and T-705**
194 BHK-21 cells were seeded together with RABV-HEP (MOI = 0.01) into
195 serially diluted NHC and T-705 in 96-well plates. After 4 days post-infection,
196 cells were stained with MTT and lysed with 2-propanol containing 10% Triton X
197 and 0.28% HCl. Cell viabilities in each well were then calculated based on the
198 absorbance at 570 nm. The absorbance of infected cells without antiviral
199 treatment and uninfected cells without antiviral treatment served as the baseline

for 0% and 100% cell viability, respectively. Combination index (CI) values, isobologram plots and criteria of combination effect were analyzed as previously described (Chou and Talalay, 1984; Fukao et al., 2018). In brief, CI values were calculated using the following formula: $CI = (D_{A/A+B})/D_A + (D_{B/A+B})/D_B + (D_{A/A+B} \times D_{B/A+B})/(D_A \times D_B)$. D_A is the EC_{50} of NHC, D_B is the EC_{50} of T-705, $D_{A/A+B}$ is the concentration of NHC producing 50% inhibition in combination with T-705, and $D_{B/A+B}$ is the concentration of T-705 producing 50% inhibition in combination with NHC. In isobologram plots, $(D_{A/A+B})/D_A$ was plotted on the x-axis and $(D_{B/A+B})/D_B$ was plotted on the y-axis. The combination effect was determined by the following criteria: $CI \leqq 0.8$, synergy; $0.8 < CI < 1.2$, additive; $CI \geqq 1.2$ antagonism.

2.9 Evaluation of the antiviral efficacy of MPV in mice

All animal experiments were approved by the Institutional Animal Care and Use Committee of Hokkaido University (approval no. 19-0014, 20-0060). For RABV experiments, 6-week-old male Slc:ddY mice (Japan SLC) were infected intramuscularly with the RABV-CVS strain (5.0×10^5 FFU/head). MPV and T-705 were suspended in 0.5% (w/v) methylcellulose containing 5% (v/v) DMSO. Mice were orally administered a vehicle, MPV (500 mg/kg), T-705 (500 mg/kg) or T-705 (500 mg/kg) + MPV (500 mg/kg) suspensions 1 day before infection (q.d.). These compounds were administered 4 h before infection and then twice a day until 5- or 7-days post infection (dpi; b.i.d.). For SARS-CoV-2 experiments,

30–50-week-old female BALB/c mice (CLEA Japan) were infected intranasally with the SARS-CoV-2 MA-P10 strain (2.3×10^2 $TCID_{50}$/head). Both the vehicle control and MPV were administered b.i.d. for 5 days at 1,000 mg/kg/day. The humane endpoint was applied when body weight loss exceeded 20% compared to that on the day of infection or if severe paralysis occurred. All procedures were performed under anesthesia with three types of mixed agents (0.03 mg/mL medetomidine hydrochloride, 3 mg/mL alfaxalone, 0.5 mg/mL butorphanol tartrate in PBS) or isoflurane.

2.10 Viral load titration in the mouse brain

The brains of RABV-CVS–infected mice collected at 5 dpi were homogenized (10% w/v) in PBS. Following centrifugation, the viral titers in the supernatants were measured using the focus-forming assay.

2.11 Statistical analyses

All statistical tests were performed using Prism version 9.5.1 (GraphPad, La Jolla, CA, USA). Statistical significance was determined by one-way analysis of variance (ANOVA) with Dunnett's *post hoc* test, one-way ANOVA with Tukey's test, the log-rank (Mantel–Cox) test, Fisher's exact test and Student's *t*-test.

3 Results

3.1 NHC inhibits RABV infection in neuronal cells

To examine the anti-RABV activity of NHC, NA cells were infected with RABV-CVS and treated with NHC. RABV-CVS, a laboratory fixed strain, exhibits *in vivo* pathogenicity and propagates efficiently in cell lines (Takahashi et al., 2020) and this strain is frequently used in antiviral drug research (Anindita et al., 2018; Xie et al., 2023; Yamada et al., 2016). As such we intentionally and primarily used the RABV-CVS strain in our studies. Treatment with NHC decreased viral titers in the culture supernatants and intracellular viral RNA levels at 48 hpi in a dose-dependent manner (Fig. 1A, B). Immunofluorescence images also revealed that treatment with NHC reduced RABV N protein production (Fig. 1C). Next, we investigated the antiviral effects of NHC against other RABV strains. Treatment with NHC also reduced the viral titers of both the attenuated fixed strain RABV-HEP and the street strain RABV-Toyohashi (Fig. 1D, E). These findings suggest that NHC suppresses RABV propagation in mouse neuroblastoma cells independent of viral strain.

3.2 NHC exhibits comparable anti-RABV activity as RBV and T-705 *in vitro*

It has been reported that the nucleoside analogs RBV and T-705 have antiviral activity against RABV (Du Pont et al., 2019) . We compared the anti-RABV-CVS activity of NHC, RBV, and T-705 based on viral titer reduction in various cell lines. Treatment with NHC, RBV, and T-705 decreased viral titers in a dose-dependent manner, and the EC_{90}s of these compounds were closely comparable

266 in N2a and BHK-21 cells (Fig. 2A, B, Table 1). NHC and RBV, but not T-705,
267 displayed antiviral activity against RABV in NA cells, which lack the metabolic
268 enzyme HPRT required for T-705 activation (Fig. S1A, Table 1) (Yamada et al.,
269 2016). Among the nucleoside analogs examined, NHC exhibited the lowest EC_{90}
270 and decreased viral titers in a dose dependent manner in SK-N-SH cells (Fig. 2C,
271 Table 1). We also confirmed the low cytotoxicity of these compounds using the
272 MTT assay (Table 1). Collectively, these results indicated that the antiviral
273 activity of NHC against RABV infection is comparable to those of RBV and T-
274 705 in neuronal and nonneuronal cell lines.
275

276 3.3 **NHC inhibits RABV replication at the post-entry stage**
277 To determine which stage in the viral life cycle is targeted by NHC, we
278 performed a time-of-addition assay (Fig. 3A). GRP-60367, a RABV entry
279 inhibitor (Du Pont et al., 2020), was employed as a control in this assay. GRP-
280 60367 suppressed viral RNA expression more strongly when administered as
281 treatment at pre-entry than after virus inoculation (Fig. 3B). The antiviral effect
282 of RBV was higher in the post-entry treatment compared to the pre-entry
283 treatment, as has been reported previously (Fig. 3B)(Anindita et al., 2018). In
284 addition, post-entry treatment with T-705 significantly reduced viral RNA levels
285 compared to both the pre-entry treatment and the non-treated condition (Fig. 3B).
286 Similarly, the addition of NHC at 1 hpi significantly decreased viral RNA levels,
287 whereas NHC treatment prior to infection had no inhibitory effect on RABV

infection (Fig. 3B). These results indicated that NHC inhibited RABV replication at a post-entry stage.

3.4 MPV exhibits no efficacy against RABV-infected mice in a prophylactic model

To assess the *in vivo* efficacy of NHC, we used MPV, an orally bioavailable prodrug of NHC, to treat RABV-infected mice. Mice prophylactically received a vehicle, T-705, or MPV orally 1 day prior to infection. The following day, mice were infected with RABV-CVS intramuscularly and orally treated b.i.d. with each compound for 5 days (Fig. 4A). In the survival analysis, all mice in the vehicle group developed lethal infection by 7 dpi, but four of six mice (67%) survived in the T-705 treatment group (Fig. 4B). In contrast, all mice treated with MPV succumbed and survival was not prolonged (Fig. 4B). Brain viral titers at 5 dpi were lower in the T-705 group than in the vehicle group. However, the titers in the MPV group were comparable to those in the vehicle group (Fig. 4C). To examine whether MPV was metabolized to its active form for the antiviral effect in mice, we administered MPV to mice infected with mouse-adapted SARS-CoV-2 (Fig. S2A). Mice treated with MPV exhibited reduced body weight loss and protection against lethal infection by SARS-CoV-2 (Fig. S2B, C). Since the efficacy of MPV monotherapy was limited, we investigated the possibility of combination therapy of MPV with T-705. First, we examined the *in vitro* combination effect of NHC with T-705 using a CPE-based assay previously

reported (Uemura et al., 2023). The isobologram resulted in CI of 1.1, indicating that the *in vitro* combination effect of NHC and T-705 was additive (Fig. S3A). Next, we examined the effect of combination treatment with T-705 and MPV on mice infected with RABV-CVS. There was no significant difference in survival between mice receiving T-705 monotherapy and combination therapy with T-705 and MPV (Fig. S3B). Taken together, no antiviral effects of MPV against RABV infection were observed in our *in vivo* experiments.

4 Discussion

Rabies is a fatal neurological disorder with no established treatment. Therefore, the development of antiviral drugs with anti-RABV activity are urgently required. NHC has displayed effectiveness against certain viruses of the order *Mononegavirales*. However, no reports have described its efficacy against *Rhabdoviridae* viruses. In the present study, we found for the first time that NHC exhibited anti-RABV activity *in vitro*. Given reports that NHC is converted into its active 5′-triphosphate form in the brain (Painter et al., 2019), NHC would be expected to exert antiviral effects in neuronal cell lines. Treatment with NHC inhibited RABV-CVS infection in neuronal and nonneuronal cells in a dose-dependent manner. To confirm that clinically isolated RABV is susceptible to NHC, we also included the RABV Toyohashi strain in this study(Nosaki et al., 2021) , demonstrating that NHC has antiviral activity against both fixed and street strains. These results indicate that NHC exhibits antiviral activity against RABV infection *in vitro* regardless of the viral strain.

Previous studies indicated that NHC primarily inhibits virus replication through mutagenesis within viral genomes (Kabinger et al., 2021; Urakova et al., 2018). The result of the time-of-addition assay illustrated that NHC inhibits the RABV replication at the post-entry stage. In animal experiments, prophylactic treatment with T-705 improved the survival rate and reduced the viral titer in the brains of RABV-infected mice, confirming its effectiveness. Conversely, prophylactic administration of MPV did not prolong survival in mice or reduce viral titers in the brain. Although 1000 mg/kg/day is the maximum MPV concentration that can be administered continuously without body weight loss (Painter et al., 2019), high-dose MPV treatment did not result in comparable efficacy as that of T-705 *in vivo*. In addition, the therapeutic effect of combined treatment with T-705 and MPV was comparable to that of T-705 alone in RABV-CVS–infected mice. Previous reports revealed that the concentration of NHC in the brain is approximately 10-fold lower than in the spleen and lungs in both mice and hamsters (Lieber et al., 2022; Painter et al., 2019). In contrast, T-705 has been reported to accumulate in the brain to the same extent as that observed in other tissues in hamsters (Gowen et al., 2015). The lower delivery of MPV to the CNS would seem to be related to the poor outcome of MPV treatment in RABV-infected mice. Indeed, treatment with MPV also failed to improve the survival rate or decrease viral titers in mice infected with La Crosse virus, which directly invades the CNS(Ojha et al., 2023) . Conversely, MPV reduced viral titers in the brain and prolonged survival in a VEEV infection mouse model (Painter et al., 2019). Treatment with 10 μM NHC reduced the viral titer by approximately one million-fold in VEEV infected cells (Urakova et al.,

2018). The *in vitro* efficacy of NHC against VEEV is stronger than that against RABV, which might be one reason why NHC is effective in the VEEV infection model. Collectively, the potential of NHC in the treatment of viral encephalitis requires further investigation.

In summary, NHC displayed efficacy against RABV *in vitro*, but not *in vivo*. The limitations for rabies treatment have constrained drug development, making the pursuit of new treatments challenging. Nucleoside analogs, known for their broad-spectrum antiviral activities, present promising treatment options for addressing such neglected diseases as rabies (Klug et al., 2016) . We conclude that NHC has potential for the initial treatment of RABV, but additional therapeutics which might be used both singly and/or in combination therapy are required to ensure clinical effectiveness once infection has involved the central nervous system.

Acknowledgments

We thank the National Institute of Infectious Diseases, Japan for providing the SARS-CoV-2 and RABV-HEP. This work was supported in part by Japan Society for the Promotion of Science (JSPS) KAKENHI under Grant number 23H02376; Japan Agency for Medical Research and Development (AMED) under Grant number JP243fa627005; Japan Science and Technology Agency (JST) Moonshot R&D under Grant number JPMJMS2025; Ministry of Health, Labour and Welfare (MHLW) under Grant number JPMH19HA1008.

Data Availability statement

Data will be made available on request.

Competing interests

All experiments reported in this paper was financially supported by Shionogi & Co., Ltd.
The authors K.K., S.K., S.T. and A.S. are employees of Shionogi & Co., Ltd. The remaining authors declare no competing interests.

CRediT authorship contribution statement

Kei Konishi: Writing –original draft, Visualization, Validation, Methodology, Investigation, Formal analysis, Data curation, Conceptualization. Shinji Kusakabe: Writing –review & editing, Methodology. Nijiho Kawaguchi: Writing –review & editing, Investigation. Takao Shishido: Writing –review & editing, Funding acquisition. Naoto Ito Writing –review & editing, Resources. Michiko Harada: Writing –review & editing, Resources. Satoshi Inoue: Writing –review & editing, Resources. Ken Maeda: Writing –review & editing, Resources. William W. Hall: Writing –review & editing. Yasuko Orba: Writing –review & editing, Funding acquisition, Supervision, Resources, Project administration. Hirofumi Sawa: Writing –review & editing, Funding acquisition, Supervision, Resources, Project administration. Michihito Sasaki: Writing –review & editing, Methodology, Investigation, Funding acquisition, Supervision, Resources, Project administration, Conceptualization. Akihiko Sato: Writing –review & editing, Methodology, Investigation, Funding acquisition, Supervision, Resources, Project administration, Conceptualization.

398

399 **References**

400

401 Anindita, P.D., Sasaki, M., Okada, K., Ito, N., Sugiyama, M., Saito-Tarashima, N., Minakawa,
402 N., Shuto, S., Otsuguro, S., Ichikawa, S., Matsuda, A., Maenaka, K., Orba, Y. & Sawa, H.,
403 2018. Ribavirin-related compounds exert in vitro inhibitory effects toward rabies virus.
404 Antiviral Res. 154, 1-9. https://doi.org/10.1016/j.antiviral.2018.03.011.
405 Appolinario, C.M. & Jackson, A.C., 2015. Antiviral Therapy for Human Rabies. Antivir. Ther.
406 20, 1-10. https://doi.org/10.3851/imp2851.
407 Arslan, F. & Vahaboglu, H., 2023. An Update to the Critical Appraisal of Milwaukee Protocol.
408 World J Surg Surgical Res. 6, 1471. https://doi.org/10.25107/2637-4625.1471.
409 Banyard, A.C., Mansfield, K.L., Wu, G., Selden, D., Thorne, L., Birch, C., Koraka, P.,
410 Osterhaus, A. & Fooks, A.R., 2019. Re-evaluating the effect of Favipiravir treatment on
411 rabies virus infection. Vaccine 37, 4686-4693. https://doi.org/10.1016/j.vaccine.2017.10.109.
412 Beigel, J.H., Tomashek, K.M., Dodd, L.E., Mehta, A.K., Zingman, B.S., Kalil, A.C.,
413 Hohmann, E., Chu, H.Y., Luetkemeyer, A., Kline, S., Lopez de Castilla, D., Finberg, R.W.,
414 Dierberg, K., Tapson, V., Hsieh, L., Patterson, T.F., Paredes, R., Sweeney, D.A., Short, W.R.,
415 Touloumi, G., Lye, D.C., Ohmagari, N., Oh, M.D., Ruiz-Palacios, G.M., Benfield, T.,
416 Fätkenheuer, G., Kortepeter, M.G., Atmar, R.L., Creech, C.B., Lundgren, J., Babiker, A.G.,
417 Pett, S., Neaton, J.D., Burgess, T.H., Bonnett, T., Green, M., Makowski, M., Osinusi, A.,
418 Nayak, S. & Lane, H.C., 2020. Remdesivir for the Treatment of Covid-19 - Final Report. N.
419 Engl. J. Med. 383, 1813-1826. https://doi.org/10.1056/NEJMoa2007764.
420 Bluemling, G.R., Mao, S., Natchus, M.G., Painter, W., Mulangu, S., Lockwood, M., De La
421 Rosa, A., Brasel, T., Comer, J.E., Freiberg, A.N., Kolykhalov, A.A. & Painter, G.R., 2023.

422 The prophylactic and therapeutic efficacy of the broadly active antiviral ribonucleoside N(4)-
423 Hydroxycytidine (EIDD-1931) in a mouse model of lethal Ebola virus infection. Antiviral
424 Res. 209, 105453. https://doi.org/10.1016/j.antiviral.2022.105453.
425 Bussereau, F., Picard, M., Blancou, J. & Sureau, P., 1988. Treatment of rabies in mice and
426 foxes with antiviral compounds. Acta Virol. 32, 33-49.
427 Butler, C.C., Hobbs, F.D.R., Gbinigie, O.A., Rahman, N.M., Hayward, G., Richards, D.B.,
428 Dorward, J., Lowe, D.M., Standing, J.F., Breuer, J., Khoo, S., Petrou, S., Hood, K., Nguyen-
429 Van-Tam, J.S., Patel, M.G., Saville, B.R., Marion, J., Ogburn, E., Allen, J., Rutter, H., Francis,
430 N., Thomas, N.P.B., Evans, P., Dobson, M., Madden, T.A., Holmes, J., Harris, V., Png, M.E.,
431 Lown, M., van Hecke, O., Detry, M.A., Saunders, C.T., Fitzgerald, M., Berry, N.S.,
432 Mwandigha, L., Galal, U., Mort, S., Jani, B.D., Hart, N.D., Ahmed, H., Butler, D., McKenna,
433 M., Chalk, J., Lavallee, L., Hadley, E., Cureton, L., Benysek, M., Andersson, M., Coates, M.,
434 Barrett, S., Bateman, C., Davies, J.C., Raymundo-Wood, I., Ustianowski, A., Carson-Stevens,
435 A., Yu, L.M. & Little, P., 2023. Molnupiravir plus usual care versus usual care alone as early
436 treatment for adults with COVID-19 at increased risk of adverse outcomes (PANORAMIC):
437 an open-label, platform-adaptive randomised controlled trial. Lancet 401, 281-293.
438 https://doi.org/10.1016/s0140-6736(22)02597-1.
439 Chou, T.C. & Talalay, P., 1984. Quantitative analysis of dose-effect relationships: the
440 combined effects of multiple drugs or enzyme inhibitors. Adv. Enzyme Regul. 22, 27-55.
441 https://doi.org/10.1016/0065-2571(84)90007-4.
442 Downs, I.L., David Ordonez Luna, A., Kota, K.P., Rubin, S.K., Shirsekar, S.S., Ward, M.D.,
443 Panchal, R.G. & Litosh, V.A., 2023. Modification of N-hydroxycytidine yields a novel lead
444 compound exhibiting activity against the Venezuelan equine encephalitis virus. Bioorg. Med.
445 Chem. Lett. 94, 129432. https://doi.org/10.1016/j.bmcl.2023.129432.

446 Du Pont, V., Plemper, R.K. & Schnell, M.J., 2019. Status of antiviral therapeutics against
447 rabies virus and related emerging lyssaviruses. Curr. Opin. Virol. 35, 1-13.
448 https://doi.org/10.1016/j.coviro.2018.12.009.
449 Du Pont, V., Wirblich, C., Yoon, J.J., Cox, R.M., Schnell, M.J. & Plemper, R.K., 2020.
450 Identification and Characterization of a Small-Molecule Rabies Virus Entry Inhibitor. J. Virol.
451 94, e00321-00320. https://doi.org/10.1128/jvi.00321-20.
452 Ehteshami, M., Tao, S., Zandi, K., Hsiao, H.M., Jiang, Y., Hammond, E., Amblard, F., Russell,
453 O.O., Merits, A. & Schinazi, R.F., 2017. Characterization of β-d-N(4)-Hydroxycytidine as a
454 Novel Inhibitor of Chikungunya Virus. Antimicrob. Agents Chemother. 61, e02395-02316.
455 https://doi.org/10.1128/aac.02395-16.
456 Fooks, A.R., Cliquet, F., Finke, S., Freuling, C., Hemachudha, T., Mani, R.S., Müller, T.,
457 Nadin-Davis, S., Picard-Meyer, E., Wilde, H. & Banyard, A.C., 2017. Rabies. Nat Rev Dis
458 Primers 3, 17091. https://doi.org/10.1038/nrdp.2017.91.
459 Fukao, K., Noshi, T., Yamamoto, A., Kitano, M., Ando, Y., Noda, T., Baba, K., Matsumoto,
460 K., Higuchi, N., Ikeda, M., Shishido, T. & Naito, A., 2018. Combination treatment with the
461 cap-dependent endonuclease inhibitor baloxavir marboxil and a neuraminidase inhibitor in a
462 mouse model of influenza A virus infection. J. Antimicrob. Chemother. 74, 654-662.
463 https://doi.org/10.1093/jac/dky462.
464 Geraghty, R.J., Aliota, M.T. & Bonnac, L.F., 2021. Broad-Spectrum Antiviral Strategies and
465 Nucleoside Analogues. Viruses 13, 667. https://doi.org/10.3390/v13040667.
466 Gowen, B.B., Sefing, E.J., Westover, J.B., Smee, D.F., Hagloch, J., Furuta, Y. & Hall, J.O.,
467 2015. Alterations in favipiravir (T-705) pharmacokinetics and biodistribution in a hamster
468 model of viral hemorrhagic fever. Antiviral Res. 121, 132-137.
469 https://doi.org/10.1016/j.antiviral.2015.07.003.

Henry, R.E., Blanton, J.D., Angelo, K.M., Pieracci, E.G., Stauffer, K., Jentes, E.S., Allen, J., Glynn, M., Brown, C.M., Friedman, C.R. & Wallace, R., 2022. A country classification system to inform rabies prevention guidelines and regulations. J. Travel Med. 29, taac046. https://doi.org/10.1093/jtm/taac046.

Imran, M., Kumar Arora, M., Asdaq, S.M.B., Khan, S.A., Alaqel, S.I., Alshammari, M.K., Alshehri, M.M., Alshrari, A.S., Mateq Ali, A., Al-Shammeri, A.M., Alhazmi, B.D., Harshan, A.A., Alam, M.T. & Abida, 2021. Discovery, Development, and Patent Trends on Molnupiravir: A Prospective Oral Treatment for COVID-19. Molecules 26, 5795. https://doi.org/10.3390/molecules26195795.

Itakura, Y., Tabata, K., Saito, T., Intaruck, K., Kawaguchi, N., Kishimoto, M., Torii, S., Kobayashi, S., Ito, N., Harada, M., Inoue, S., Maeda, K., Takada, A., Hall, W.W., Orba, Y., Sawa, H. & Sasaki, M., 2023. Morphogenesis of Bullet-Shaped Rabies Virus Particles Regulated by TSG101. J. Virol. 97, e0043823. https://doi.org/10.1128/jvi.00438-23.

Jayk Bernal, A., Gomes da Silva, M.M., Musungaie, D.B., Kovalchuk, E., Gonzalez, A., Delos Reyes, V., Martín-Quirós, A., Caraco, Y., Williams-Diaz, A., Brown, M.L., Du, J., Pedley, A., Assaid, C., Strizki, J., Grobler, J.A., Shamsuddin, H.H., Tipping, R., Wan, H., Paschke, A., Butterton, J.R., Johnson, M.G. & De Anda, C., 2022. Molnupiravir for Oral Treatment of Covid-19 in Nonhospitalized Patients. N. Engl. J. Med. 386, 509-520. https://doi.org/10.1056/NEJMoa2116044.

Kabinger, F., Stiller, C., Schmitzová, J., Dienemann, C., Kokic, G., Hillen, H.S., Höbartner, C. & Cramer, P., 2021. Mechanism of molnupiravir-induced SARS-CoV-2 mutagenesis. Nat. Struct. Mol. Biol. 28, 740-746. https://doi.org/10.1038/s41594-021-00651-0.

Kimitsuki, K., Khan, S., Kaimori, R., Yahiro, T., Saito, N., Yamada, K., Nakajima, N., Komeno, T., Furuta, Y., Quiambao, B.P., Virojanapirom, P., Hemachudha, T. & Nishizono,

494 A., 2023. Implications of the antiviral drug favipiravir on rabies immunoglobulin for post-
495 exposure prophylaxis of rabies in mice model with category III-like exposures. Antiviral Res.
496 209, 105489. https://doi.org/10.1016/j.antiviral.2022.105489.
497 Klug, D.M., Gelb, M.H. & Pollastri, M.P., 2016. Repurposing strategies for tropical disease
498 drug discovery. Bioorg. Med. Chem. Lett. 26, 2569-2576.
499 https://doi.org/10.1016/j.bmcl.2016.03.103.
500 Lawitz, E., Mangia, A., Wyles, D., Rodriguez-Torres, M., Hassanein, T., Gordon, S.C.,
501 Schultz, M., Davis, M.N., Kayali, Z., Reddy, K.R., Jacobson, I.M., Kowdley, K.V., Nyberg,
502 L., Subramanian, G.M., Hyland, R.H., Arterburn, S., Jiang, D., McNally, J., Brainard, D.,
503 Symonds, W.T., McHutchison, J.G., Sheikh, A.M., Younossi, Z. & Gane, E.J., 2013.
504 Sofosbuvir for Previously Untreated Chronic Hepatitis C Infection. N. Engl. J. Med. 368,
505 1878-1887. https://doi.org/10.1056/nejmoa1214853.
506 Lieber, C.M., Cox, R.M., Sourimant, J., Wolf, J.D., Juergens, K., Phung, Q., Saindane, M.T.,
507 Smith, M.K., Sticher, Z.M., Kalykhalov, A.A., Natchus, M.G., Painter, G.R., Sakamoto, K.,
508 Greninger, A.L. & Plemper, R.K., 2022. SARS-CoV-2 VOC type and biological sex affect
509 molnupiravir efficacy in severe COVID-19 dwarf hamster model. Nat Commun 13, 4416.
510 https://doi.org/10.1038/s41467-022-32045-1.
511 Nosaki, Y., Maeda, K., Watanabe, M., Yokoi, T., Iwai, K., Noguchi, A., Tobiume, M., Satoh,
512 M., Kaku, Y., Sato, Y., Kato, H., Okutani, A., Kawahara, M., Harada, M., Inoue, S., Maeda,
513 K., Suzuki, T., Saijo, M. & Takayama-Ito, M., 2021. Fourth imported rabies case since the
514 eradication of rabies in Japan in 1957. J. Travel Med. 28, taab151.
515 https://doi.org/10.1093/jtm/taab151.
516 Ojha, D., Hill, C.S., Zhou, S., Evans, A.B., Leung, J.M., Lewis, C.S., Amblard, F., Schinazi,
517 R.F., Baric, R.S., Peterson, K.E. & Swanstrom, R., 2023. N(4) -

518 Hydroxycytidine/Molnupiravir Inhibits RNA-Virus Induced Encephalitis by Producing
519 Mutated Viruses with Reduced Fitness. bioRxiv. https://doi.org/10.1101/2023.08.22.554316.
520 Painter, G.R., Bowen, R.A., Bluemling, G.R., DeBergh, J., Edpuganti, V., Gruddanti, P.R.,
521 Guthrie, D.B., Hager, M., Kuiper, D.L., Lockwood, M.A., Mitchell, D.G., Natchus, M.G.,
522 Sticher, Z.M. & Kolykhalov, A.A., 2019. The prophylactic and therapeutic activity of a
523 broadly active ribonucleoside analog in a murine model of intranasal venezuelan equine
524 encephalitis virus infection. Antiviral Res. 171, 104597.
525 https://doi.org/10.1016/j.antiviral.2019.104597.
526 Sanderson, T., Hisner, R., Donovan-Banfield, I.a., Hartman, H., Løchen, A., Peacock, T.P. &
527 Ruis, C., 2023. A molnupiravir-associated mutational signature in global SARS-CoV-2
528 genomes. Nature 623, 594-600. https://doi.org/10.1038/s41586-023-06649-6.
529 Sreenivasan, N., Li, A., Shiferaw, M., Tran, C.H., Wallace, R., Blanton, J., Knopf, L., Abela-
530 Ridder, B. & Hyde, T., 2019. Overview of rabies post-exposure prophylaxis access,
531 procurement and distribution in selected countries in Asia and Africa, 2017-2018. Vaccine 37
532 Suppl 1, A6-a13. https://doi.org/10.1016/j.vaccine.2019.04.024.
533 Sugiyama, M., Ito, N., Minamoto, N. & Tanaka, S., 2002. Identification of immunodominant
534 neutralizing epitopes on the hemagglutinin protein of rinderpest virus. J. Virol. 76, 1691-
535 1696. https://doi.org/10.1128/jvi.76.4.1691-1696.2002.
536 Takahashi, T., Inukai, M., Sasaki, M., Potratz, M., Jarusombuti, S., Fujii, Y., Nishiyama, S.,
537 Finke, S., Yamada, K., Sakai, H., Sawa, H., Nishizono, A., Sugiyama, M. & Ito, N., 2020.
538 Genetic and Phenotypic Characterization of a Rabies Virus Strain Isolated from a Dog in
539 Tokyo, Japan in the 1940s. Viruses 12, 914. https://doi.org/10.3390/v12090914.
540 Uemura, K., Nobori, H., Sato, A., Toba, S., Kusakabe, S., Sasaki, M., Tabata, K., Matsuno,
541 K., Maeda, N., Ito, S., Tanaka, M., Anraku, Y., Kita, S., Ishii, M., Kanamitsu, K., Orba, Y.,

542 Matsuura, Y., Hall, W.W., Sawa, H., Kida, H., Matsuda, A. & Maenaka, K., 2023. 2-
543 thiouridine is a broad-spectrum antiviral nucleoside analogue against positive-strand RNA
544 viruses. Proc. Natl. Acad. Sci. U. S. A. 120, e2304139120.
545 https://doi.org/10.1073/pnas.2304139120.
546 Urakova, N., Kuznetsova, V., Crossman, D.K., Sokratian, A., Guthrie, D.B., Kolykhalov,
547 A.A., Lockwood, M.A., Natchus, M.G., Crowley, M.R., Painter, G.R., Frolova, E.I. & Frolov,
548 I., 2018. β-d-N(4)-Hydroxycytidine Is a Potent Anti-alphavirus Compound That Induces a
549 High Level of Mutations in the Viral Genome. J. Virol. 92, e01965-01917.
550 https://doi.org/10.1128/jvi.01965-17.
551 Venkataraman, S., Prasad, B. & Selvarajan, R., 2018. RNA Dependent RNA Polymerases:
552 Insights from Structure, Function and Evolution. Viruses 10, 76.
553 https://doi.org/10.3390/v10020076.
554 Willoughby, R.E., Jr., Tieves, K.S., Hoffman, G.M., Ghanayem, N.S., Amlie-Lefond, C.M.,
555 Schwabe, M.J., Chusid, M.J. & Rupprecht, C.E., 2005. Survival after treatment of rabies with
556 induction of coma. N. Engl. J. Med. 352, 2508-2514.
557 https://doi.org/10.1056/NEJMoa050382.
558 Xie, Y., Chi, Y.L., Liu, S.Q. & Zhu, W.Y., 2023. BCX4430 inhibits the replication of rabies
559 virus by suppressing mTOR-dependent autophagy invitro. Virology 585, 21-31.
560 https://doi.org/10.1016/j.virol.2023.05.012.
561 Yamada, K., Noguchi, K., Komeno, T., Furuta, Y. & Nishizono, A., 2016. Efficacy of
562 Favipiravir (T-705) in Rabies Postexposure Prophylaxis. J. Infect. Dis. 213, 1253-1261.
563 https://doi.org/10.1093/infdis/jiv586.
564 Yoon, J.J., Toots, M., Lee, S., Lee, M.E., Ludeke, B., Luczo, J.M., Ganti, K., Cox, R.M.,
565 Sticher, Z.M., Edpuganti, V., Mitchell, D.G., Lockwood, M.A., Kolykhalov, A.A., Greninger,

A.L., Moore, M.L., Painter, G.R., Lowen, A.C., Tompkins, S.M., Fearns, R., Natchus, M.G. & Plemper, R.K., 2018. Orally Efficacious Broad-Spectrum Ribonucleoside Analog Inhibitor of Influenza and Respiratory Syncytial Viruses. Antimicrob. Agents Chemother. 62, e00766-00718. https://doi.org/10.1128/aac.00766-18.

Zeiler, F.A. & Jackson, A.C., 2016. Critical Appraisal of the Milwaukee Protocol for Rabies: This Failed Approach Should Be Abandoned. Can. J. Neurol. Sci. 43, 44-51. https://doi.org/10.1017/cjn.2015.331.

Figure legends

Fig. 1. Antiviral efficacy of NHC against RABV infection in mouse neuroblastoma cells

(A–C) NA cells were inoculated with RABV-CVS at a MOI of 0.01 for 1 h and then cultured with NHC-containing medium. Viral titers in supernatants (A) were determined by the focus-forming assay, and viral RNA (B) was analyzed by qRT-PCR. Images of immunofluorescence staining present RABV N protein (green) and nuclei (blue)(C). Scale bars, 100 μm. **(D–E)** NA cells were inoculated with RABV-HEP at a MOI of 0.01 (D) or RABV-Toyohashi at a MOI of 0.1 (E) for 1 h and cultured with NHC-containing medium for 48 h. Viral titers in supernatants were determined by focus-forming assays. Experiments (A, B, D, and E) were performed in triplicate, and the data are representative of two independent experiments. Data are presented as the mean ± SD. Statistical analysis was performed by one-way ANOVA with Dunnett's *post hoc* test to compare with non-treated cells. *$p < 0.05$, **$p < 0.01$, ***$p < 0.001$, ****$p < 0.0001$.

589 **Fig. 2. Comparison of the effects of antiviral nucleoside analogs against RABV**
590 **infection in neuronal and nonneuronal cells**
591 **(A-C)** N2a (A), BHK-21 (B), and SK-N-SH (C) cells were inoculated with RABV-CVS at
592 a MOI of 0.01 for 1 h and then cultured with medium containing NHC (left), RBV
593 (middle), or T-705 (right). Each compound was evaluated in two-fold serial dilutions from
594 25 μM to 0.781 μM in N2a and BHK-21 cells, and from 50 μM to 3.13 μM in SK-N-SH
595 cells. Viral titers in supernatants were determined by the focus-forming assay. Experiments
596 were performed in triplicate, and the data are representative of two independent
597 experiments. Data are presented as the mean ± SD. Statistical analysis was performed by
598 one-way ANOVA with Dunnett's *post hoc* test to compare with non-treated cells. *$p <$
599 0.05, **$p < 0.01$, ***$p < 0.001$, ****$p < 0.0001$.
600
601 **Fig. 3. Time-of-addition assay for NHC**
602 **(A)** Schematic representation of the experimental design of the time-of-addition assay. The
603 virus inocula was preincubated with or without compounds for 1 h. For the entry
604 conditions, the virus was inoculated into N2a cells in the presence of the compounds and
605 thereafter cultured without the compounds. For the post entry conditions, the virus was
606 initially inoculated into N2a cells for 1 h without any compounds and subsequently cultured
607 in the presence of the compounds. Intracellular RNA was extracted at 16 hpi, and qRT-PCR
608 was conducted. (**B**) The relative viral RNA levels of RABV-CVS–infected N2a cells
609 treated with 25 μM NHC, 20 μM GRP-60367, 5 μM RBV or 50 μM T-705 are shown. Data
610 were normalized to those for mouse *Actb*. Experiments were performed in triplicate, and

611 the data are representative of two independent experiments. Data are presented as the mean
612 ± SD. Statistical analysis was performed by one-way ANOVA with Tukey's test. *$p < 0.05$,
613 ***$p < 0.001$, ****$p < 0.0001$.
614
615 **Fig. 4. *In vivo* efficacy of MPV in RABV-CVS–infected mice**
616 **(A)** Schematic representation of the experimental design of the prophylactic administration
617 model. Administration of vehicle, MPV, or T-705 to mice commenced 1 day prior to
618 infection (q.d., 500 mg/kg/day). On the day of infection, the compounds were administered
619 4 h before infection and daily thereafter until 5 dpi (b.i.d., 1,000 mg/kg/day). Mice were
620 infected intramuscularly with RABV-CVS (5×10^5 FFU/head). Infected mice were
621 observed daily until 14 dpi; im, intramuscularly. mpk, milligram per kilogram. po, oral
622 administration. **(B, C)** Survival rates (B) and viral titers in the brain at 5 dpi (C) in RABV-
623 CVS–infected mice treated with vehicle, MPV, or T-705 (n = 6 for survival rate analysis, n
624 = 8 for viral titer analysis). Each plot indicates the individual viral titers of infected mice.
625 The dashed line indicates the lower limit of detection, and gray dots denote data that were
626 below the lower limit of detection. Bar, median. Statistical analysis was performed by the
627 log-rank (Mantel–Cox) test (B) or Fisher's exact test (C). *p* values were adjusted by the
628 Bonferroni correction. *$p < 0.05$, **$p < 0.01$.

Table 1

Antiviral activity, cytotoxicity, and selective index (SI_{90}) of NHC, RBV and T-705 against RABV-CVS strain. EC_{90} (μM), the concentration of antiviral compound that reduced the virus titer by 90% relative to non-treated control. CC_{50} (μM), the concentration that reduced cell viability by 50% relative to the DMSO-treated control. SI_{90} is the ratio of CC_{50} to EC_{90} (CC_{50}/EC_{90}). Experiments were performed in triplicate and these data are representative of two independent experiments. n.d. : not determined

	NHC			RBV			T-705		
	EC_{90}	CC_{50}	SI_{90}	EC_{90}	CC_{50}	SI_{90}	EC_{90}	CC_{50}	SI_{90}
NA	7.4	165.9	22.4	2.4	69.7	29.0	>100.0	>200	n.d.
N2a	6.4	>200	>31.3	11.3	174.2	15.4	9.6	>200	>20.8
BHK-21	9.2	171.0	18.6	8.6	>200	>23.2	9.3	>200	>21.5
SK-N-SH	18.1	>200	>11	>100.0	>200	n.d.	>100.0	>200	n.d.

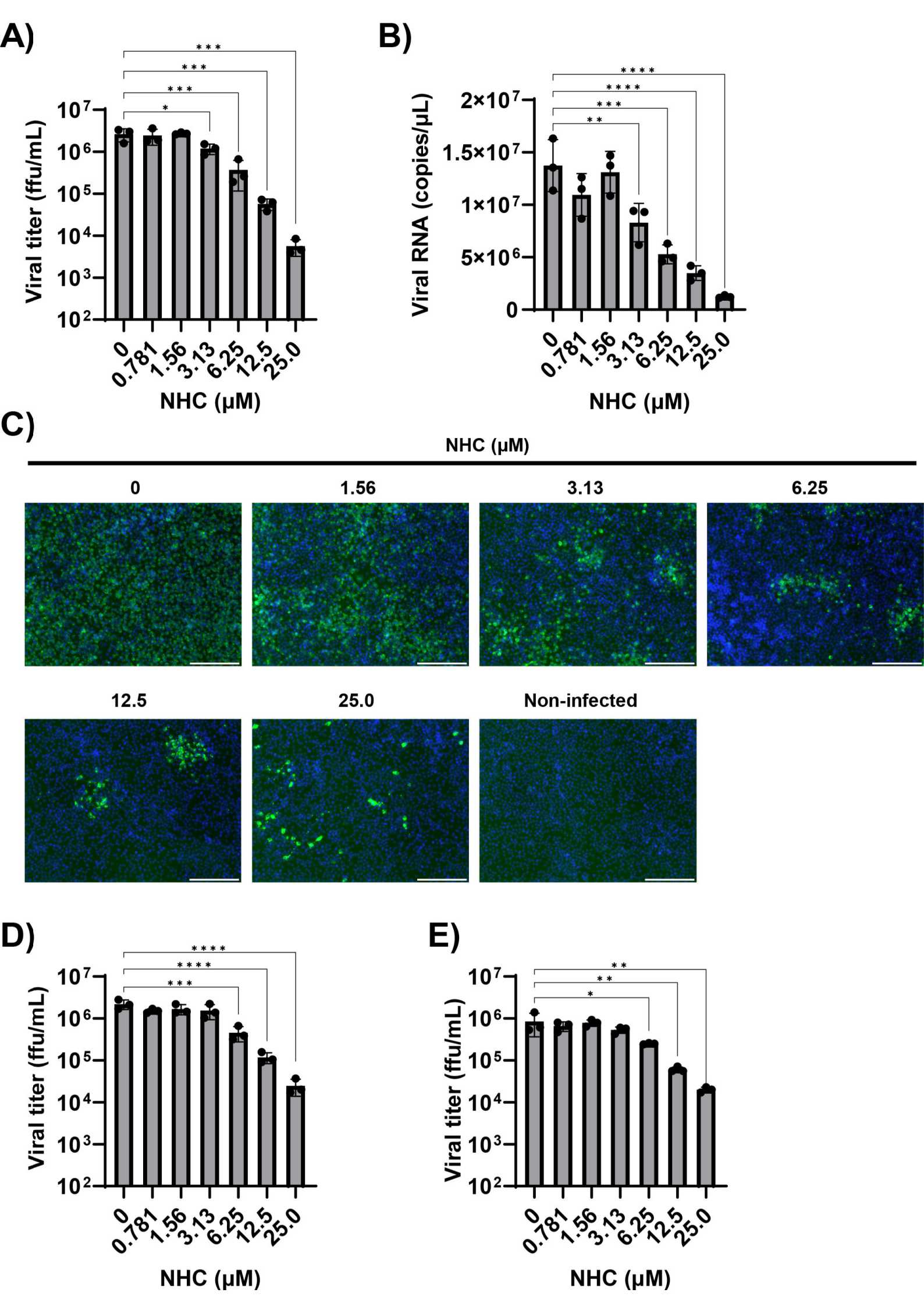
A)
Viral titer (ffu/mL)
NHC (μM)
B)
Viral RNA (copies/μL)
NHC (μM)
C)
NHC (μM)
0
1.56
3.13
6.25
12.5
25.0
Non-infected
D)
Viral titer (ffu/mL)
NHC (μM)
E)
Viral titer (ffu/mL)
NHC (μM)

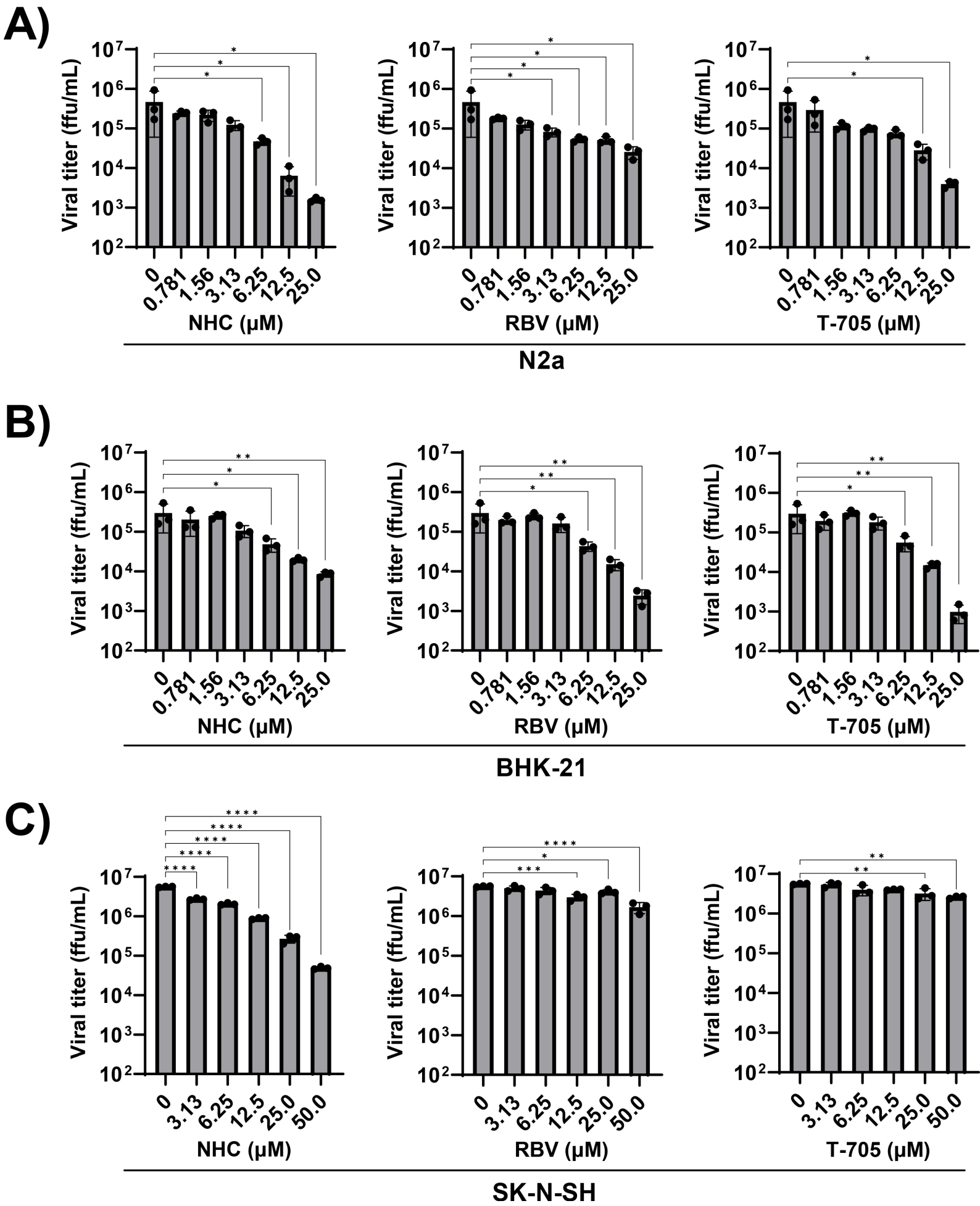
A)
Viral titer (ffu/mL)
NHC (μM)
RBV (μM)
T-705 (μM)
N2a
B)
BHK-21
C)
SK-N-SH

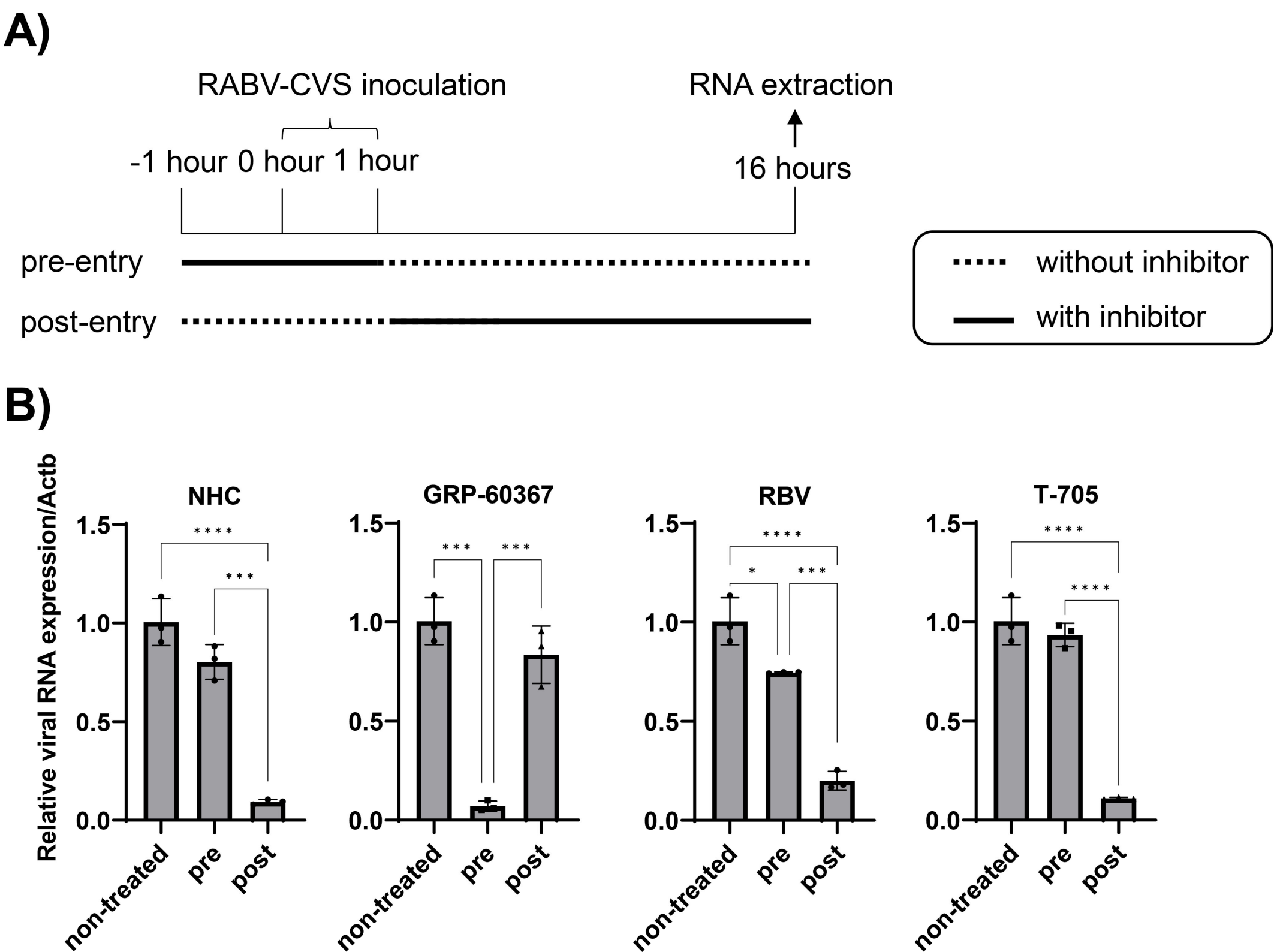
A)
RABV-CVS inoculation
RNA extraction
-1 hour 0 hour 1 hour
16 hours
pre-entry
post-entry
without inhibitor
with inhibitor
B)
Relative viral RNA expression/Actb
NHC
GRP-60367
RBV
T-705
1.5
1.0
0.5
0.0
****
***
*
non-treated
pre
post

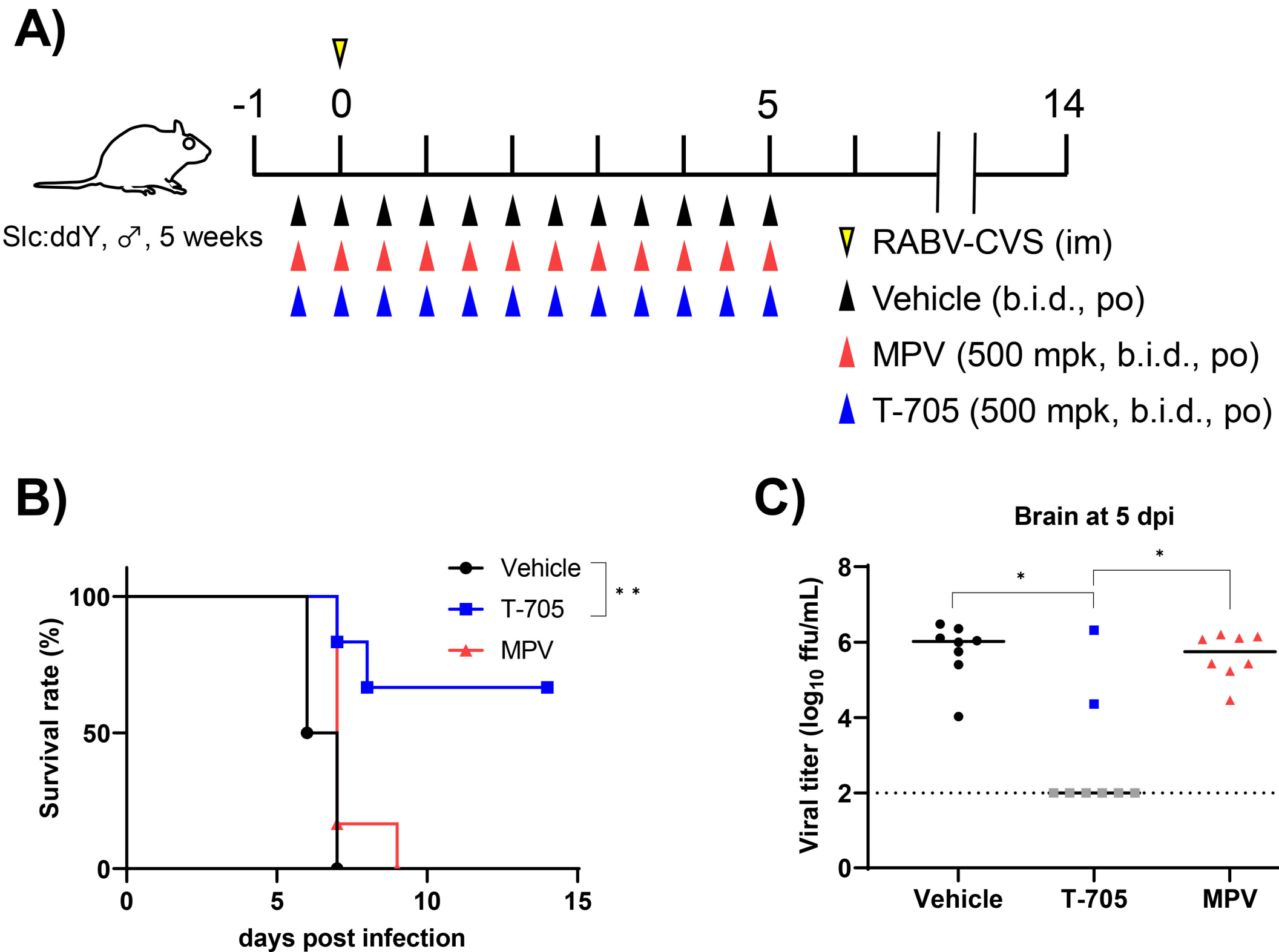
A)
-1
0
5
14
Slc:ddY, ♂, 5 weeks
RABV-CVS (im)
Vehicle (b.i.d., po)
MPV (500 mpk, b.i.d., po)
T-705 (500 mpk, b.i.d., po)
B)
Survival rate (%)
100
50
0
0
5
10
15
days post infection
Vehicle
T-705
MPV
* *
C)
Brain at 5 dpi
Viral titer (log10 ffu/mL)
8
6
4
2
0
*
*
Vehicle
T-705
MPV